

DOI: 10.1515/amm-2017-0265

M. AKBARZADEH\*, M. ZANDRAHIMI\*<sup>#</sup>, E. MORADPOUR\*\*

## MOLYBDENUM DISULFIDE (MoS<sub>2</sub>) COATING ON AISI 316 STAINLESS STEEL BY THERMO-DIFFUSION METHOD

Molybdenum disulfide (MoS<sub>2</sub>) is one of the most widely used solid lubricants applied in different ways on the surfaces under friction. In this work, AISI 316 austenitic stainless steel was coated with MoS<sub>2</sub>, using thermo-diffusion method at different temperatures and times. Coatings properties were investigated using SEM, EDX, XRD and FTIR, Hardness Tester and Roughness tester. The results illustrated the formation of a uniform layer on the surface, containing MoS<sub>2</sub> and MoO<sub>3-x</sub> phases. The thickness, grain size and the hardness of the coatings were 20-50 μm, 400-1000 nm and 350- 550 HV respectively. Friction tests carried out using ball-on-disc method under normal loads of 10 N under ambient conditions showed values of the friction coefficient 0.30-0.40. In addition, the kinetics of diffusion layers between the substrate and the coating were also investigated. It was found that there at steady temperature there is a parabolic relationship between the thickness of the diffusion layer and the treatment time. The activation energy for the process was estimated to be 143 kJ mol<sup>-1</sup>. Depending on the treatment time and temperature, the thicknesses of diffusion layer varied between 0.5 and 2.5 microns.

*Keywords:* Thermo-diffusion method, solid lubricant coating, molybdenum disulfide

### 1. Introduction

Solid lubricants are materials which despite being in the solid phase, are able to provide protection from damage during relative movement and to reduce friction and wear. They are applied either as surface coatings or as fillers in self-lubricating composites. Solid lubricant coatings are required for lubrication of moving mechanical assemblies operating in hostile environments and severe conditions like high temperature, high load, ultralow temperatures, ultrahigh vacuums, strong radiation where conventional Liquid lubrication are hardly applicable [1,2].

Transition metal di-chalcogenides MX<sub>2</sub> (X = S, Se, Te; and M = W, Mo, Nb, Ta) are one kind of solid lubricant materials that nowadays they have been widely used in industry [3,4].

Molybdenum disulfide is an excellent solid lubricant and are widely used in high-precision space-borne applications such as satellite bearings, gears, and gimbals operating under extreme temperature ranges. MoS<sub>2</sub> crystallizes in the hexagonal structure where a sheet of molybdenum atoms is sandwiched between two hexagonally packed sulfur layers. The bonding within the S–Mo–S sandwich is covalent, while weak Van der Waals forces hold the sandwich together resulting in inter lamellar mechanical weakness. Thus, Because of the weak van der Waals interactions between the sheets of sulfide atoms, MoS<sub>2</sub> has a low coefficient of friction, producing its lubricating properties [5].

Until now, a large number of methods have been developed to prepare MoS<sub>2</sub> films, that among these, PVD methods are successfully used in production of high-performance MoS<sub>2</sub> coatings. Limiting factors of the PVD technologies are their high production costs and complex equipment and slow rate of coating deposition. Also it is a line of sight technique meaning that it is extremely difficult to coat undercuts and similar surface features costs besides, deposition of an intermediate layer (e.g., TiN, TiAlN) is necessary for acceptable adhesion to steel substrates [2,6].

The thermo-diffusion synthesis is a simple method to produce thick coatings in the absence of any binding agents in the resultant coatings and have low production costs. Formation of the transition layer on the substrate coating interface allows formation of thick layers on substrates without any binding compounds [7-9].

The goal of the presented work is to study the MoS<sub>2</sub> Solid lubricants coatings formed on AISI 316 austenitic stainless steel substrates by thermo-diffusion Method.

### 2. Experimental

Coupons of AISI 316L stainless steel, measuring 10 mm ×5 mm×2 mm, with chemical composition of 17.4% Cr, 2% Mn,

\* SHAHID BAHONAR UNIVERSITY OF KERMAN, FACULTY OF ENGINEERING, DEPARTMENT OF METALLURGY AND MATERIALS SCIENCE, JOMHOORI ESLAMI BLVD., KERMAN, IRAN

\*\* SANAAT RESEARCH INSTITUTE, TEHRAN, IRAN

<sup>#</sup> Corresponding author: m.zandrahimi@mail.uk.ac.ir

1% Si, 0.08% C, 0.02% S, with Fe as remaining were used as substrates. Specimens were polished from 320-grit sic paper up to 1200-grit, ultrasonically cleaned in ethanol and then dried. In order to deposit  $\text{MoS}_2$  onto the substrate, the thermo-diffusion method was employed. This method consists of two stages. During the first stage (“molybdizing”) samples were immersed into the fine  $\text{MoO}_3$  powder with average particle size of 0.4, 2 and 20  $\mu\text{m}$  and are heated in Argon atmosphere. This stage ensures adherence of  $\text{MoO}_3$  powder to the sample and thick  $\text{MoO}_3$  coating is formed. Molybdizing stage carried out at different temperatures (650–750°C for different times (2–8h).

The second stage (‘sulfurizing’) is performed in special stainless steel chamber (Fig. 1) in the sulfur vapor atmosphere. In this stage oxygen displacement by sulfur.

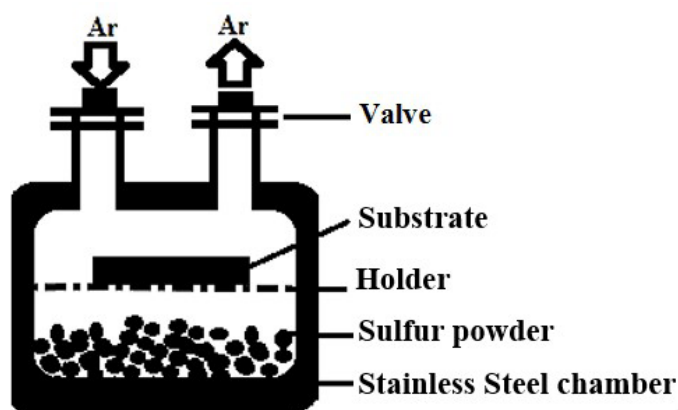


Fig. 1. A schematic elastration of sulfurizing chamber

In order to avoid sulfur vapor deposition during chamber cooling, the surfaces of samples were covered by a layer of molybdenum (IV) sulfur powder (<2  $\mu\text{m}$ ). Then chamber was heated in the shaft furnace at 650, 700 and 750°C for 4h.

Microstructure and chemical composition of the surface and cross section of coatings were analyzed using scanning electron microscopy (SEM) (Camscan MV2300) with energy dispersive spectroscopy (EDS). IR spectra were recorded in the 400–4000  $\text{cm}^{-1}$  range with a resolution of 4  $\text{cm}^{-1}$ , using Bruker tensor 27 FTIR spectrometer with RT-DLATGS detector and KBr pellet technique X-ray diffraction (XRD) were used to identify the phases that formed in the surface layer of the as-coated, using  $\text{Cu K}\alpha$  radiation ( $\lambda = 1.5405 \text{ \AA}$ ). Phase identification and Rietveld quantitative phase analysis were carried out using the XPert High Score Plus v2.2 software.

The crystallite size was evaluated from the X-ray diffraction patterns based on the Scherrer formula that is defined as:

$$\beta \cos \theta = K \lambda / d \quad 1$$

Where  $\beta$  is the line broadening at half the maximum intensity (FWHM) in radians,  $\lambda$  is the wavelength,  $\theta$  is the diffraction angle, and  $d$  is crystallite size [10].

The surface roughness was measured using stylus type (Talysurf Taylor Hobson) instruments. The average surface roughness was measured at five different locations and results were averaged.

Friction tests were performed using a pin-on-disk machine. This equipment is controlled by its PC software, which allows observing the evolution of the friction coefficient. During the test, the treated samples were rotating against a stationary AISI 52100 steel pin (with 4.576 mm hemispherical tip radius and hardness of 800 HV30) at a linear speed of 0.11 m/s under loads of 10 N.

### 3. Results

Fig. 2 shows SEM images of coating after molybdizing stage at 600 and 750°C. Coating fabricated at 600°C has many

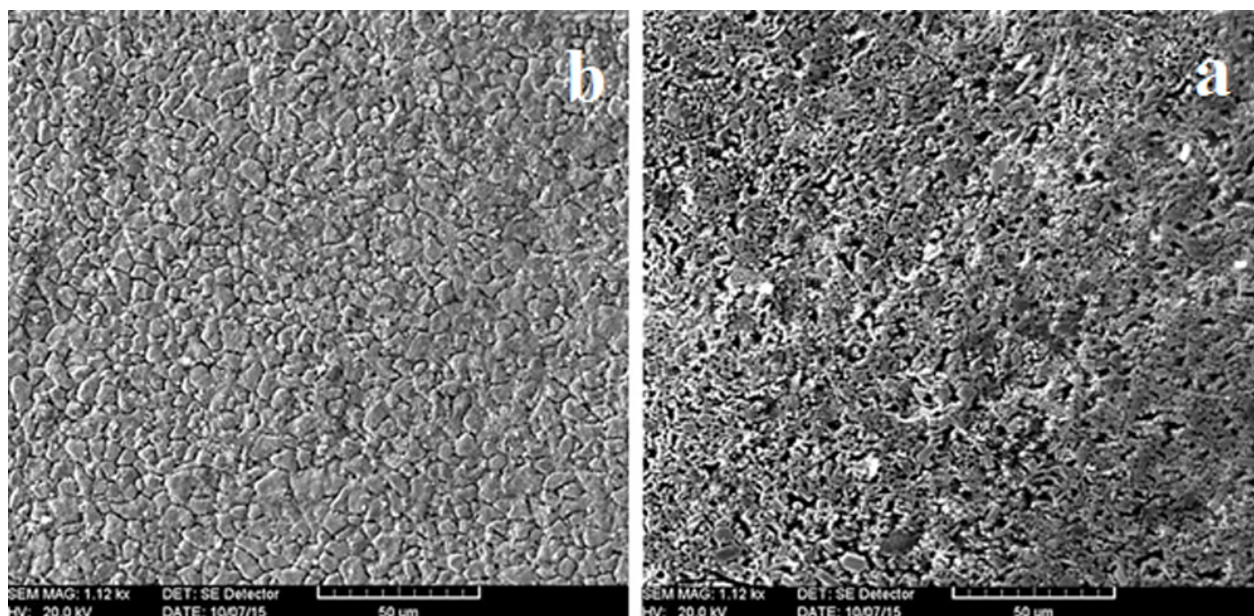


Fig. 2. SEM images of  $\text{MoO}_3$  coating prepared at different temperatures deposition; (a) 600°C and (b) 750°C

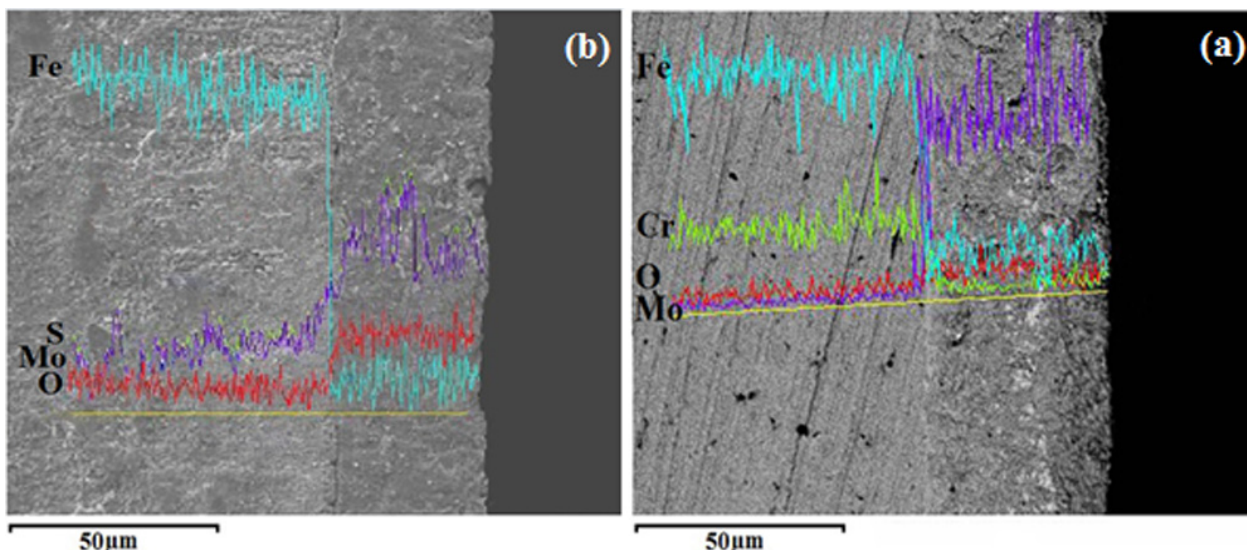


Fig. 3. SEM image of the specimen cross-section and distribution of Fe, Mo, O and S elements (a) after molibdzizing stage (b) after sulfurizing stage

pores and large voids. It was suggested that there may be inadequate diffusion of molybdenum to steel at 650°C, resulting in discontinuities in the coatings. But as can be seen in Fig. 2b Coating fabricated at 750°C is integrated, uniform continuous and without porosity. Diffusive embedding of molybdenum into substrate takes place during 750°C which results in formation of adherence and continues MoO<sub>3</sub> coating on substrate [8].

Fig. 3 shows a cross section SEM image and EDS line scan of a coated specimen before and after sulfurizing stage. The thickness of coatings is about 50 µm and it shows good adherence to the substrate with no voids, pores or discontinuities. Volumetric change in the coating during the sulfurizing stage was not observed, which could be explained by nearby values of density of MoO<sub>3</sub> (4.7 gr/cm<sup>3</sup>) and MoS<sub>2</sub> (4.8 gr/cm<sup>3</sup>). So Thickness of the resultant coating is controlled by parameters of the molibdzizing stage such as temperature and duration of the molibdzizing.

The temperature of molibdzizing is usually within 550-750°C. Higher temperatures result in lateral cracks and lon-

gitudinal spalling; Lower temperatures usually bring about an inadequate adhesion and significant residual porosity.

In thermo-diffusion method, the thickness of coatings may vary from several microns to tens of microns depending on the process parameters. So it can be strictly controlled by temperature and duration of the treatment. Formation of the transition layer between substrate and coating allows formation of thick MoS<sub>2</sub> layers on steel without any binding compounds. Transition layer can be observed in concentration EDX profiles of molybdenum, iron, sulfur and oxygen across the coating (from the steel substrate depth to the coating surface) as shown in Fig. 3. The Transition area is diffusion layer where molybdenum content increase and iron content decrease. The graphical representation in Fig. 5 shows that diffusion layer thickness increases with the treatment time at each process temperature and varies with time as a parabolic law as follows:

$$\frac{x^2}{t} = k \quad 1$$

Where  $x$  is the diffusion layer thickness ( $\mu$ ), the treatment time ( $h$ ) and  $K$  is the diffusion coefficient ( $\mu^2 h^{-1}$ ). Mo and Fe diffusion from substrate and coating are the main factors affecting the coating layer thickness. The plot of the square of the diffusion layer thickness versus treatment time is being shown as linear in Fig. 6. The diffusion coefficient (growth rate constant),  $K$  depending on treatment temperature were calculated from the slopes of the plots (Fig. 6). The relationship between the diffusion coefficients,  $K$ , activation energy,  $Q$ , and the process temperature in Kelvin,  $T$ , can be expressed as an Arrhenius equation:

$$K = K_0 \cdot \exp\left(-\frac{Q}{RT}\right) \quad 2$$

Where  $K_0$  is the frequency factor and  $R$  is the gas constant.  $K_0$  and  $Q$  are temperature independent constants. (Eq. 3) was expressed from the natural logarithm of (Eq. 3) as follows

$$\ln K = \ln K_0 - \frac{Q}{RT} \quad 3$$

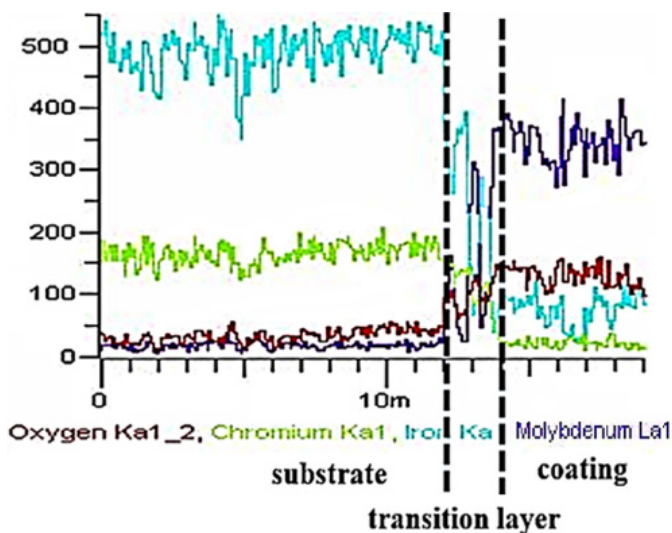


Fig. 4. EDS concentration profiles across the coating

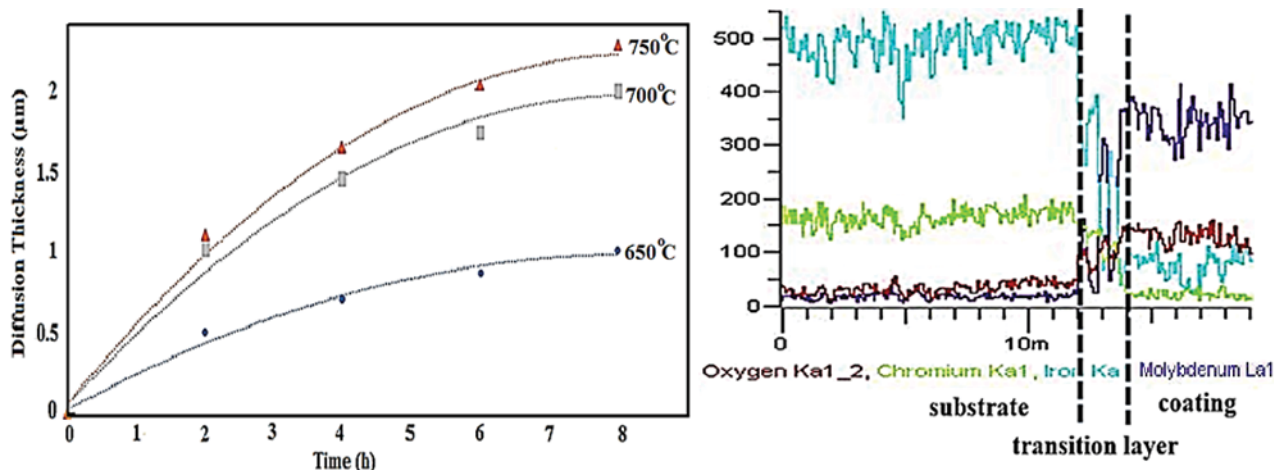


Fig. 5. Diffusion layer thickness as a function of treatment time and temperature

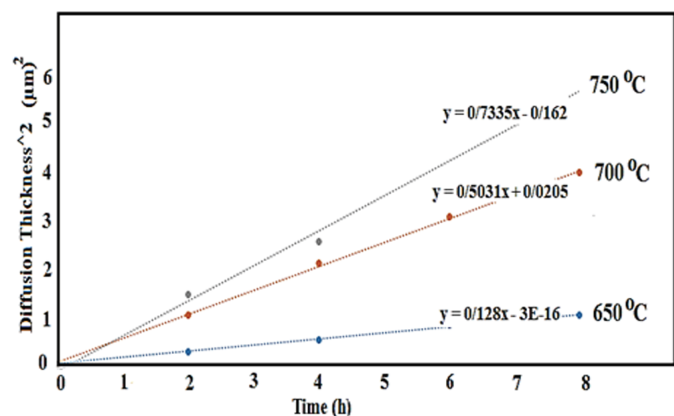


Fig. 6. Square of the diffusion layer thickness,  $y$ , vs. coating time,  $x$

The graph of  $\ln K$  versus reciprocal treatment temperature is thus being shown to be linear in Fig. 7. The activation energy,  $Q$ , was calculated by the slope of the plot ( $\ln K/T^{-1}$ ) in Fig. 7. As shown in Fig. 5, diffusion rate constant,  $K$  increases with increasing treatment temperature. Activation energy ( $Q$ ) and diffusion coefficient ( $K$ ) were determined to be  $143 \text{ kJ mol}^{-1}$  and  $12.25 \times 10^6 \mu^2 \text{ h}^{-1}$  respectively.

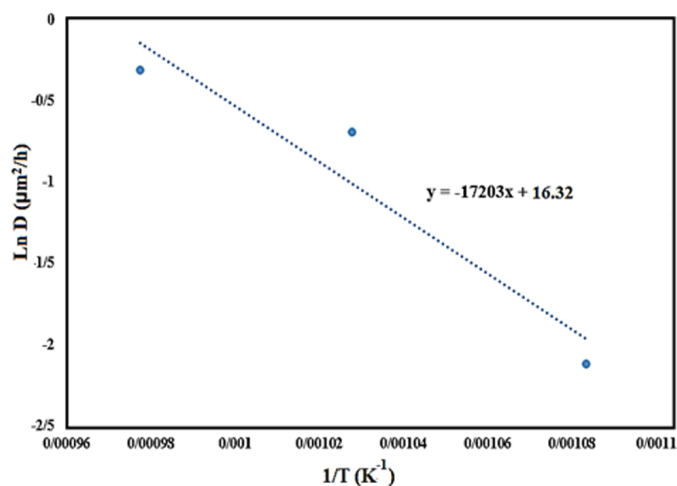


Fig. 7.  $\ln D$  vs.  $1/T$  for Diffusion layer

The derived formulas between the square layer thickness and treatment temperature is shown in (Eq. 7):

$$K = 12.25 \times 10^6 \exp\left(-\frac{17203}{T}\right) \quad 4$$

Where  $K$  is the diffusion coefficient ( $\mu^2 \text{ h}^{-1}$ ) and  $T$  is the temperature ( $K$ ). The practical formula, for calculating the layer thickness ( $m$ ) for time ( $h$ ) and temperature ( $K$ ), derived from (Eqs. 4 and 7) is seen in

$$x = 3.5 \times 10^3 \times \sqrt{t \cdot \exp\left(\frac{-17203}{T}\right)} \quad 5$$

Fig. 8 shows dependence of the diffusion layer thickness on the time and temperature parameters. As can be seen the surfaces of the coated samples have more roughness than substrate, so coating increases the surface roughness. The measured surface roughness of the coatings at different molybdizing temperatures and molybdizing temperatures particle size of  $\text{MoO}_3$  powders is given in Fig. 9. The roughness of the coatings are independent of parameters of the coating stages of thermo-diffusion method

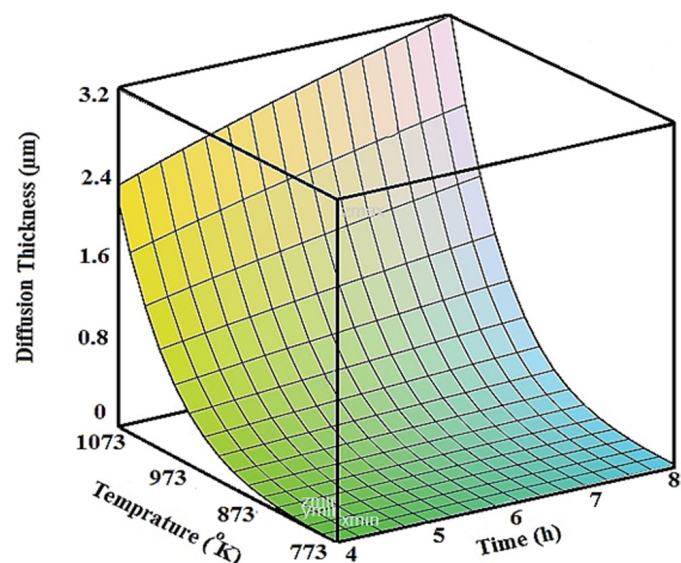


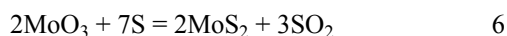
Fig. 8. Dependence of the coating thickness on the synthesis parameters

and close to the mean particle diameter of the MoO<sub>3</sub> powder in molybdizing stage.

Fig. 10 shows XRD diffraction patterns of coatings before and after of sulfurizing stages at 650, 700 and 750°C sulfurizing for 4 hour. The identified phases include MoO<sub>3</sub>, MoO<sub>3-x</sub>, MoO<sub>2</sub> and MoS<sub>2</sub>. Suboxide MoO<sub>3-x</sub> phases are intermediate and non-equilibrium phases (Mo<sub>9</sub>O<sub>26</sub>, Mo<sub>8</sub>O<sub>23</sub>, Mo<sub>4</sub>O<sub>11</sub>, Mo<sub>9</sub>O<sub>26</sub>, Mo<sub>9</sub>O<sub>25</sub>, Mo<sub>5</sub>O<sub>14</sub>, etc.) that convert into stable MoO<sub>2</sub> phase at evaluated temperature in sulfurization stage.

The strong diffraction peaks indicate that the product has good crystallinity. When the sulfurizing temperature is increased from 650°C to 750°C, these peaks are weakened slightly, indicating that the crystallinity is reduced.

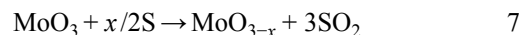
Fig. 11 shows that the phase compositions obtained by Rietveld refinement of coatings at different sulfurizing temperature. The reaction between MoO<sub>3</sub> and S is given in (Eq. 6).



Sulfurization temperature plays an important role in synthesizing MoS<sub>2</sub>. MoO<sub>3</sub> coating was reduced by the sulfur vapor to form suboxide MoO<sub>3-x</sub>, which diffused to the substrate and further reacted with sulfur vapor to grow MoS<sub>2</sub> phase. According to Fig. 8 sulfurization of MoO<sub>3</sub> could not be finished at a high

sulfurizing temperature (750°C) even for 240 min. MoO<sub>2</sub> is one of the most stable in Mo compounds, so intermediate product exists generally in form of MoO<sub>2</sub>.

With the increase of sulfurizing temperature from 600°C to 750°C, the presence of MoO<sub>2</sub> is significantly reduced and dominantly MoS<sub>2</sub> is achieved. From these experiments, it can be concluded that the reaction occurs in two phases; phase one involves sulfur vapor reducing MoO<sub>3</sub> to MoO<sub>3-x</sub> and in the second phase the excess sulfur reacts with MoO<sub>3-x</sub> and produces MoS<sub>2</sub>. Possible reaction equations can be described as follows:



The process temperature and reaction duration determine the degree of conversion of the MoO<sub>3</sub> into MoS<sub>2</sub> film [11-13].

The IR technique was used to verify the XRD assignments of oxide, sulfide species. The FT-IR spectrum of coating is shown in Fig. 12. The relatively sharp bands at 974 and 911 cm<sup>-1</sup> are ascribed to the Mo = O characteristic stretching vibration of the hexagonal phase. A broad and complex band peaked at 600 cm<sup>-1</sup> corresponds to the Mo – O vibration and the bands at 463 and

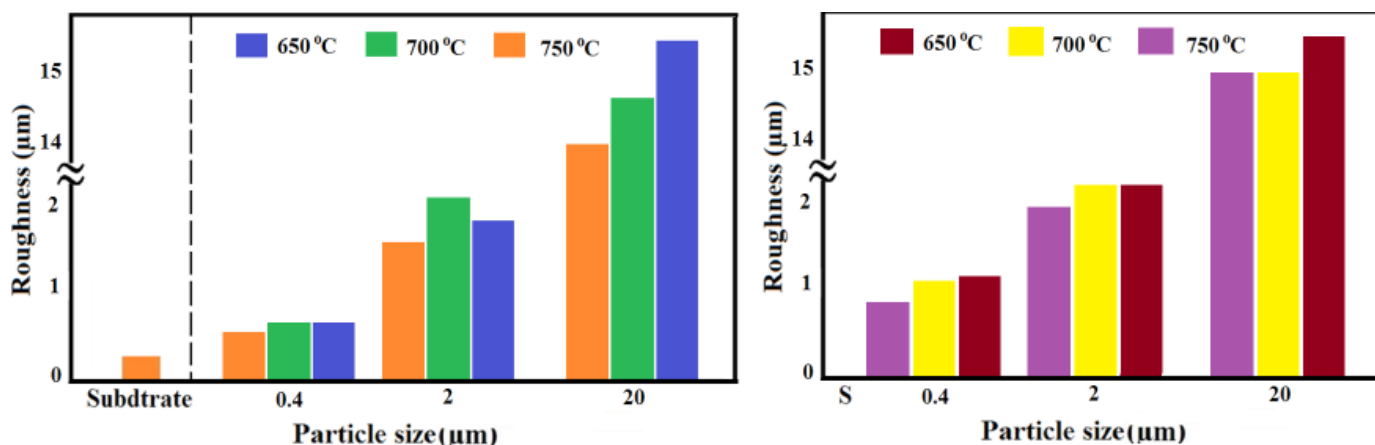


Fig. 9. Influence of average surface roughness of coatings at different particle size of MoO<sub>3</sub> powders (a) at different molybdizing temperature (a) at different sulfurizing temperature (at molybdizing temperature of 750°C)

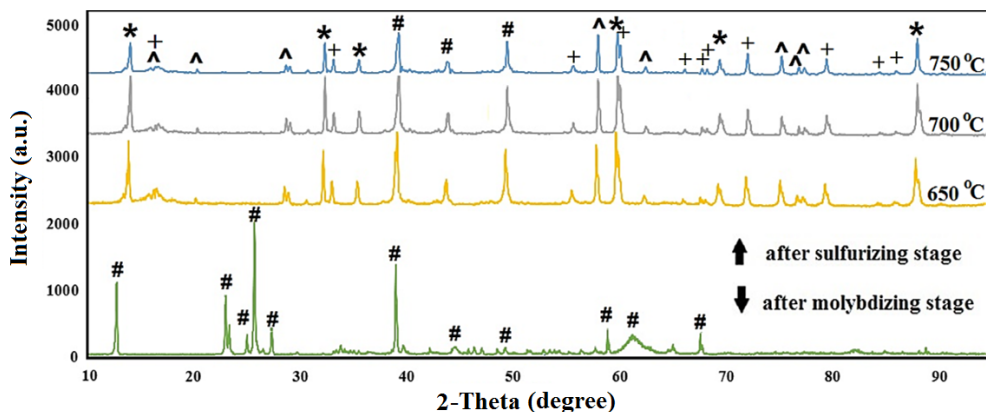


Fig. 10. XRD patterns of before and after sulfurizing stage at 650, 700 and 750°C for 180 minute (peaks correspond to [\*] MoS<sub>2</sub>, [+] MoO<sub>2</sub>, [^] MoO<sub>3-x</sub> and [#] MoO<sub>3</sub>)

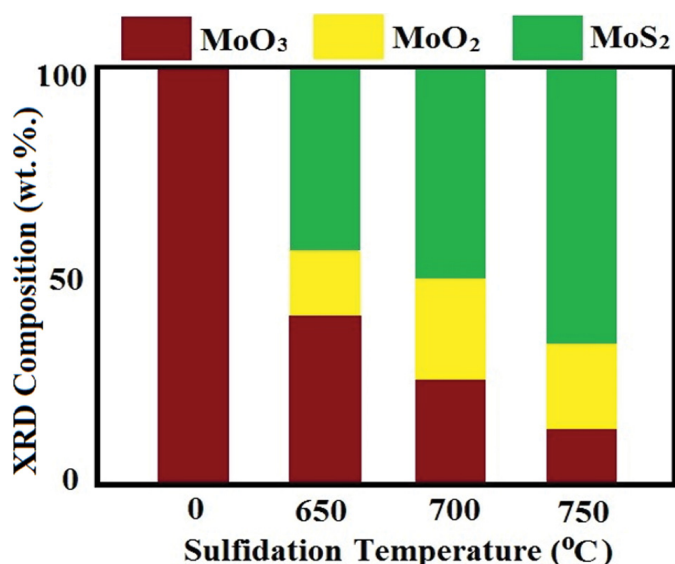


Fig. 11. Quantitative phase analysis data (wt.%) by the Rietveld Method for coatings at different sulfurizing temperature

430  $\text{cm}^{-1}$  are ascribed to the Mo = S and Mo – S characteristic stretching vibration of the hexagonal phase which matched well with reference [14-16].

Using the diffraction peaks (0 0 3) ( $2\theta = 14.05^\circ$ ) and (1 0 1) ( $2\theta = 32.80^\circ$ ) an average grain was calculated for each coating at different sulfurizing temperature.

The estimated results for all the samples are shown in Fig. 13, which clearly shows that the average grain size increases gradually as the sulfurizing temperatures increase. Combined the results of Fig. 11 and Fig. 13, it can be concluded that the grain growth dominates the phase transformation of coatings.

Fig. 14 shows the micro-Vickers hardness values of coatings at different substrate temperature. As can be seen in Fig. 14, the hardness of coatings increase with sulfurizing temperature up to a maximum of 570 HV at 700°C, then decreased progressively with increasing sulfurizing temperature. In this process phases produced and grain size of coating are two main factors that affect the hardness.

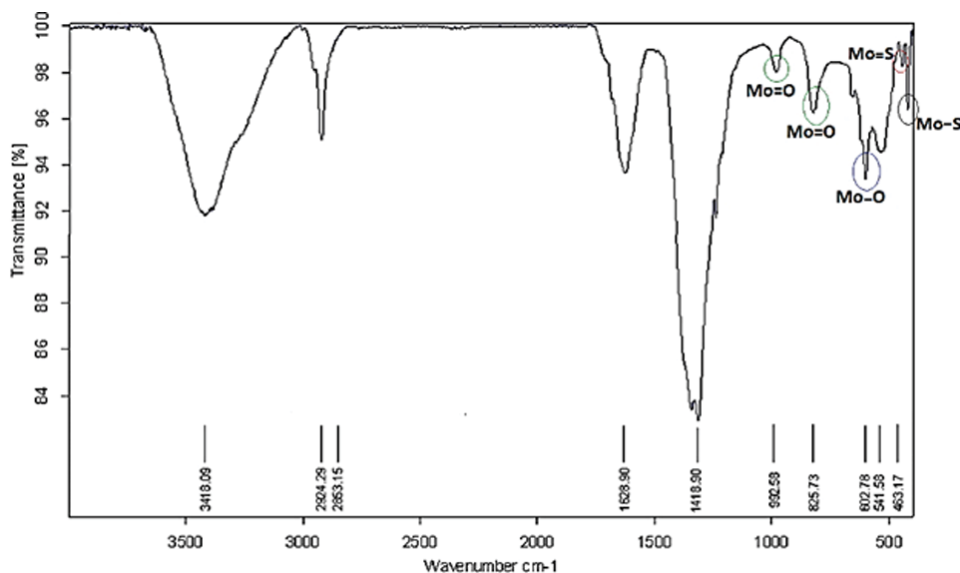


Fig. 12. FT-IR spectrum of coatings (at sulfurizing temperature of 750°C (For 4 h)

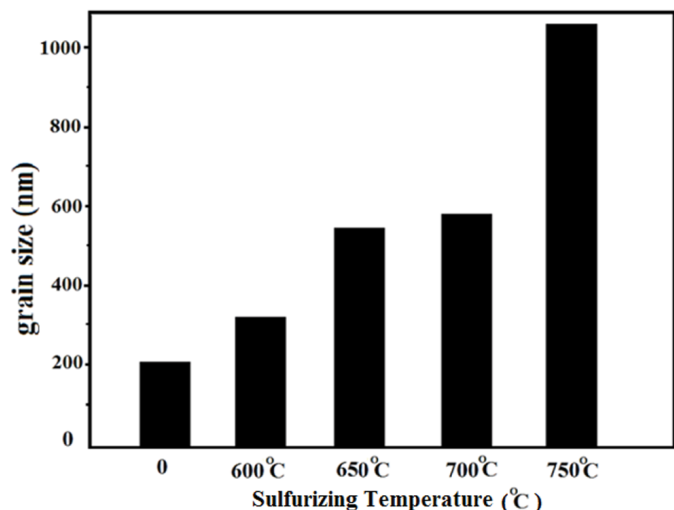


Fig. 13. The average grain size as a function of coating sulfurizing temperature

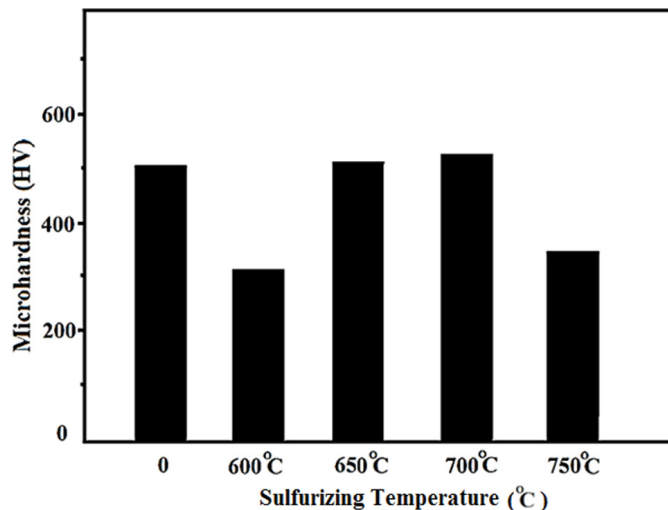


Fig. 14. The micro-Vickers hardness values of coatings at different sulfurizing temperature

The dependence of material hardness on the grain size can be described by the phenomenological “Hall-Petch” equation [17], as follows:

$$H_v = H_0 + Kd^{-0.5} \quad 9$$

Where,  $H_v$  is hardness,  $H_0$ , the term depending on the hardness of the individual grains,  $K$  a constant defining the influence of the grain boundaries and  $d$  the grain size. This relationship is based on the observation that grain boundaries impede dislocation movement and the number of dislocations within a grain have an effect on how easily dislocations can traverse grain boundaries and travel from grain to grain.

The variation of the steady state friction coefficient of the coatings and substrate is presented in Fig. 15. The average friction coefficient decreases as the sulfurizing temperatures increase. As can be seen in Fig. 11 with the increase of sulfurizing temperature the presence of  $\text{MoS}_2$  as an ultra-lubricant phase is significantly increased, so coating friction coefficient decreases with increasing sulfurizing temperature.

#### 4. Conclusions

1.  $\text{MoS}_2$  coating was successfully synthesized by thermo diffusion method onto AISI 316 stainless steel.
2. Synthesis of  $\text{MoS}_2$  coatings by Thermo Diffusion Method comprises two stages: (a) formation of the molybdenum oxide layer on the surface of the steel substrate; (b) treatment of the substrate in the vaporous sulfur environment to form  $\text{MoS}_2$ .
3. The results display the progress of  $\text{MoS}_2$  formation from  $\text{MoO}_2$  in correspondence with temperature of sulfurizing stage.
4. The coating layer has compact and dense morphology.
5. The longer the treatment time, the higher the treatment temperature, the thicker the diffusion layer became.
6. The thickness, grain size and the hardness of the coatings were 20-50  $\mu\text{m}$ , 400-1000 nm and 350-550 HV respectively.
7. Ball-on-plate tests demonstrated the coating friction coefficient 0.25-0.40 (20°C, air).

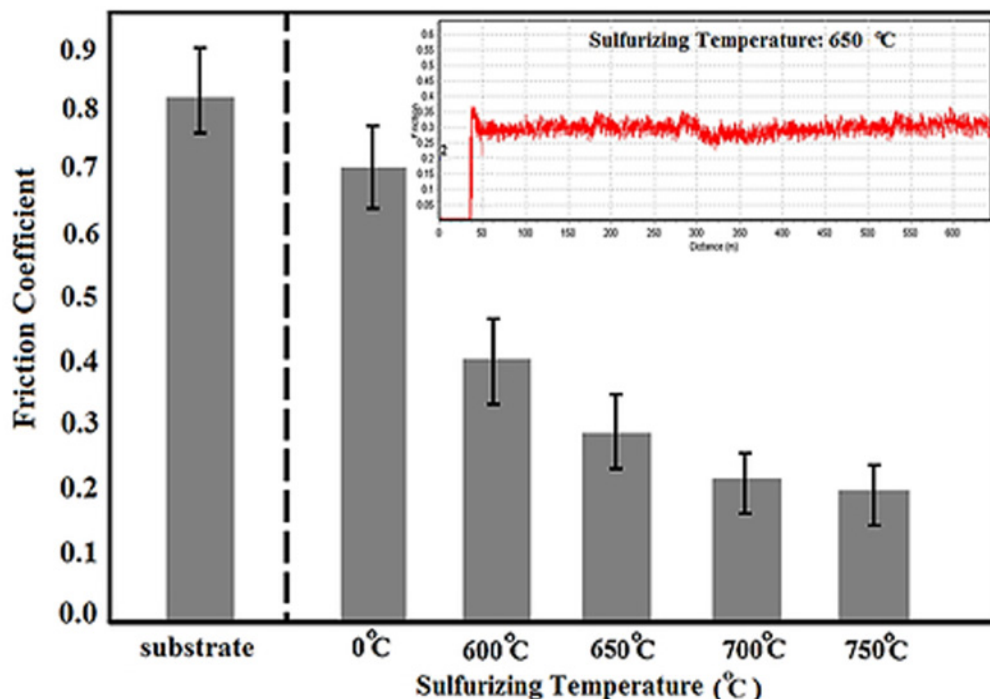


Fig. 15. The Average steady friction coefficient values of coatings at different sulfurizing temperatures

#### REFERENCES

- [1] J.-F. Yang, Y. Jiang, J. Hardell, B. Prakash, Influence of service temperature on tribological characteristics of self-lubricant coatings: A review, *Front. Mater. Sci.* **7**, 28-39 (2013).
- [2] Y. Peng, Z. Meng, C. Zhong, J. Lu, W. Yu, Y. Jia, Y. Qian, Hydrothermal Synthesis and Characterization of Single-Molecular-Layer  $\text{MoS}_2$  and  $\text{MoSe}_2$ , *Chem. Lett.* **9**, 772-773 (2001).
- [3] J.-F. Yang, B. Parakash, J. Hardell, Q.F. Fang, Tribological properties of transition metal di-chalcogenide based lubricant coatings, *Front. Mater. Sci.* **6**, 116-127 (2012).
- [4] A.B. Kaul, Graphene and two-dimensional layered materials for device applications, in: *Nanotechnology (IEEE-NANO)*, 2013 13th IEEE Conference on, IEEE, 1-4 (2013).
- [5] J.-F. Yang, Y. Jiang, J. Hardell, B. Prakash, Q.-F. Fang, Influence of service temperature on tribological characteristics of self-lubricant coatings: A review, *Front. Mater. Sci.* **7**, 28-39 (2013).
- [6] Q.J. Wang, and Y.W. Chung, *Encyclopedia of tribology: With 3650 Figures and 493 Tables*. 2013 Springer.
- [7] G.V. Karpenko, A. Aladjem, *Influence of diffusion coatings on the strength of steel*, Freund Pub. House ; Aldermansdorf, Switzerland : sole distributor, Trans Tech Publications, 1979.

- [8] O. Smorygo, S. Voronin, P. Bertrand, I. Smurov, Fabrication of thick molybdenum disulphide coatings by thermal-diffusion synthesis, *Tribol. Lett.* **17**, 723-726 (2004).
- [9] S. Voronin, O. Smorygo, P. Bertrand, I. Smurov, N. Smirnov, Y. Makarov, Thermal-diffusion synthesis of thick molybdenum disulphide coatings on steel substrates, *Surf. Coat. Technol.* **180**, 113-117 (2004).
- [10] U. Holzwarth, N. Gibson, The Scherrer equation versus the 'Debye-Scherrer equation', *Nat. Nano Technol.* **6**, 534-534 (2011).
- [11] H. Schmidt, S. Wang, L. Chu, M. Toh, R. Kumar, W. Zhao, A.H. Castro Neto, J. Martin, S. Adam, B. Ozyilmaz, Transport properties of monolayer MoS<sub>2</sub> grown by chemical vapor deposition, *Nano Lett.* **14**, 1909-1913 (2014).
- [12] Y.H. Lee, X.Q. Zhang, W. Zhang, M.T. Chang, C.T. Lin, K.D. Chang, Y.C. Yu, J.T.W. Wang, C.S. Chang, L.J. Li, Synthesis of Large-Area MoS<sub>2</sub> Atomic Layers with Chemical Vapor Deposition, *Adv. Mater.* **24**, 2320-2325 (2012).
- [13] X. Wang, H. Feng, Y. Wu, L. Jiao, Controlled synthesis of highly crystalline MoS<sub>2</sub> flakes by chemical vapor deposition, *J. Am. Chem. Soc.* **135**, 5304-5307 (2013).
- [14] I.G. Vasilyeva, I.P. Asanov, L.M. Kulikov, Experiments and Consideration about Surface Nonstoichiometry of Few-Layer MoS<sub>2</sub> Prepared by Chemical Vapor Deposition, *The Journal of Physical Chemistry C* **119**, 23259-23267 (2015).
- [15] F. Maugé, J. Lamotte, N. Nesterenko, O. Manoilo, A. Tsygankenko, FT-IR study of surface properties of unsupported MoS<sub>2</sub>, *Catal. Today* **70**, 271-284 (2001).
- [16] L.Q. Mai, B. Hu, W. Chen, Y. Qi, C. Lao, R. Yang, Y. Dai, Z.L. Wang, Lithiated MoO<sub>3</sub> nanobelts with greatly improved performance for lithium batteries, *Advanced Materials* **19**, 3712-3716 (2007).
- [17] K. Miyoshi, Y. Chung, *Surface diagnostics in tribology: Fundamental principles and applications*, World scientific, 1993.